Programming Impulsive Deformation with Mechanical Metamaterials

Xudong Liang and Alfred J. Crosby*
Polymer Science and Engineering Department, University of Massachusetts Amherst, Amherst, Massachusetts 01003, USA

(Received 23 March 2020; accepted 17 August 2020; published 2 September 2020)

Impulsive deformation is widely observed in biological systems to generate movement with high acceleration and velocity. By storing elastic energy in a quasistatic loading and releasing it through an impulsive elastic recoil, organisms circumvent the intrinsic trade-off between force and velocity and achieve power amplified motion. However, such asymmetry in strain rate in loading and unloading often results in reduced efficiency in converting elastic energy to kinetic energy for homogeneous materials. Here, we demonstrate that specific internal structural designs can offer the ability to tune quasistatic and high-speed recoil independently to control energy storage and conversion processes. Experimental demonstrations with mechanical metamaterials reveal that certain internal structures optimize energy conversion far beyond unstructured materials under the same conditions. Our results provide the first quantitative model and experimental demonstration for tuning energy conversion processes through internal structures of metamaterials.

DOI: 10.1103/PhysRevLett.125.108002

Impulsive deformation is universally adopted in biological systems to circumvent the force-velocity trade-off and exceed the power limitation of muscles [1–4]. In these systems, organisms store elastic energy in components, which serve as springs, and subsequently release this energy in a triggered recoil event. For example, the mantis shrimp powers rapid movements of its appendages (peak speed of 20 m/s) via a release of elastic energy stored in the exoskeleton [5,6], legless larvae jump 28 times their body length through a rapid release of elastic energy stored slowly through an internal pressurization process [7], and Venus flytrap leaflets couple the slow hydraulic storage of elastic energy with a snap instability to capture flying insects [8,9]. The impulsive deformation in such biological systems results from asymmetry in loading and unloading, where elastic energy is stored through quasistatic conditions and is quickly released through a fast, dynamic recoil [Fig. 1(a)]. These impulsive movements in nature are intrinsically controlled via material properties and structures. Similar approaches have been adopted in engineering systems, ranging from archery bows [10] to antibody-powered DNA nanomachines [11]. However, a systematic understanding of how structure interplays with materials properties has remained elusive for elastic recoiling structures.

Traditionally, the dynamics of recoil is linked to the coupling between the inertial and elastic properties of a system [12–14], with the recoil velocity determined by the material wave speed [15,16]. Accordingly, synthetic impulsive devices are typically tuned through the choice of the constituent material. For applications where immense power and dynamic range, hence large strains, are required, this traditional tuning approach often leads to diminishing returns. Most synthetic materials experience decreased elastic to kinetic energy conversion efficiency due to internal intrinsic dissipative mechanisms [17–19], which are amplified at high strain rates. In nature, where compositional variation is limited, it is hypothesized that structural variation can offer pathways for enhanced conversion efficiency [20–22], allowing impulsive recoil to be an advantageous adaptation for many organisms.

In this Letter, we report a strategy to overcome intrinsic limitations in impulsive deformation in homogeneous materials by utilizing mechanical metamaterials that mediate mechanically derived deformations, stresses, and energy with periodically arranged building blocks [23]. A rich set of wave dynamics, like transition waves [24] and elastic vector solitons [25,26], have been discovered in metamaterials where different internal displacement modes occur simultaneously. Here, we reveal through high-speed imaging how sequential internal displacements associated with impulsive deformation control fast motion and energy dissipation in metamaterials.

The mechanical metamaterials are composed of a network of plates connected by thin ligaments [Fig. 1(b)]. The internal structures are characterized as orthogonally aligned pores with semiminor and semimajor axes a_0 and b_0, respectively, and width of the necks between adjacent pores w_0. The representative unit used to describe the pore geometry [inset, Fig. 1(b)], has a length $L_0 = a_0 + b_0 + w_0$, with a pore aspect ratio $a_r = a_0/b_0$. The metamaterials are stretched with a global strain $\varepsilon = \Delta L/L_y$, where L_y and ΔL are the initial length and tip displacement, respectively. Ligaments respond to the global strain with a bending first, changing the shapes of the pores, and then switch to stretching at larger strain, with a_2 and b_2 being the semiminor and semimajor axes that depend on the

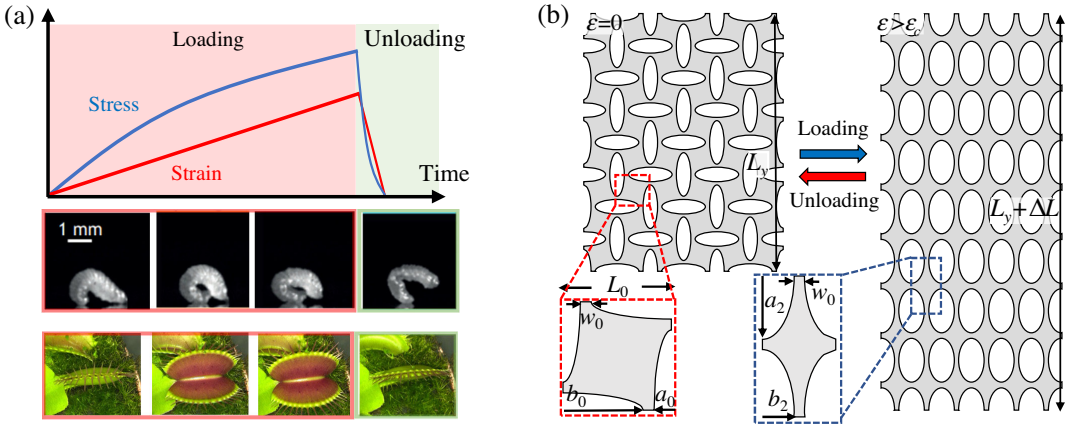

FIG. 1. (a) Asymmetric loading and unloading in jumping larvae (adapted with permission from Journal of Experimental Biology [7]) and Venus flytrap leaflets (adapted from [9]. Copyright (2011) National Academy of Sciences). (b) Mechanical metamaterials to program impulsive deformation.

global strain [27,28]. We neglect the change of ligament thickness with strain given that its variation is slight compared to other dimensions in metamaterials (Supplemental Material [29]).

The role of structure in energy storage and strain distribution was measured under quasistatic loading. The local strain is measured through the change in curvature of the ligament in bending and the change in length for the stretching ligament. The global strain required to change the ligament from bending to stretching is measured as the critical strain ε_c (Supplemental Material [29]). In Fig. 2(a), the experimentally measured ligament strain is plotted against the global strain, showing a transition of strain attenuation ($\varepsilon_l/\varepsilon < 1$) to strain concentration ($\varepsilon_l/\varepsilon > 1$) as the localized displacement changes from bending to stretching. The localized displacements also control the stiffness of the metamaterials (k), as confirmed experimentally [Fig. 2(b)]. The counterrotating motion leads to a compliant response in a metamaterial with elliptical pores ($a_r < 1$), where the thin ligaments act as a slender torsional spring. The stiffness of near-circular-pore metamaterials ($a_r \sim 1$) is governed by ligament stretching [27,32,33]. The dependence of stiffness upon pore aspect ratios contrasts to cellular solids with randomly positioned pores [29,34]. In addition, the stiffness continues decreasing after the ligament undergoes stretching due to the pore shape development with global strain [27].

The role of structure on energy release is evident in the recoiling metamaterials with circular ($a_0 = b_0$) and elliptical ($a_0 = 0.125 b_0$) pores, as captured with a high-speed camera (Photron Fastcam SA3) at 20 000 fps [Fig. 3(a)]. At time $t = 0$ ms, recoiling initiates with an elastic wave propagating along the y direction from a vertically hung sample without any external planar guiding constraints. The deformation in the circular-pore metamaterial is manifested by translational retraction of the ligaments, while the deformation of the elliptically structured sample is dominated by the rotation of the interconnecting plates (Videos S1 and S2, Supplemental Material [29]). Out-of-plane bending is suppressed during

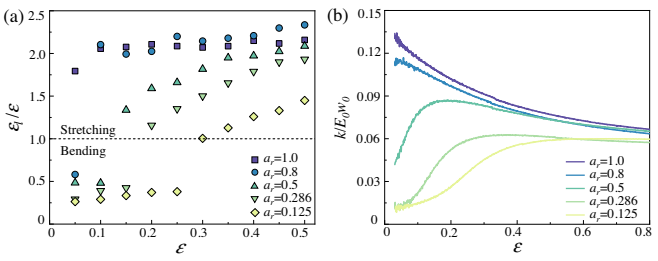

FIG. 2. (a) Maximum local strain in the ligaments in stretching. (b) Normalized stiffness of the metamaterials with different pore aspect ratios.

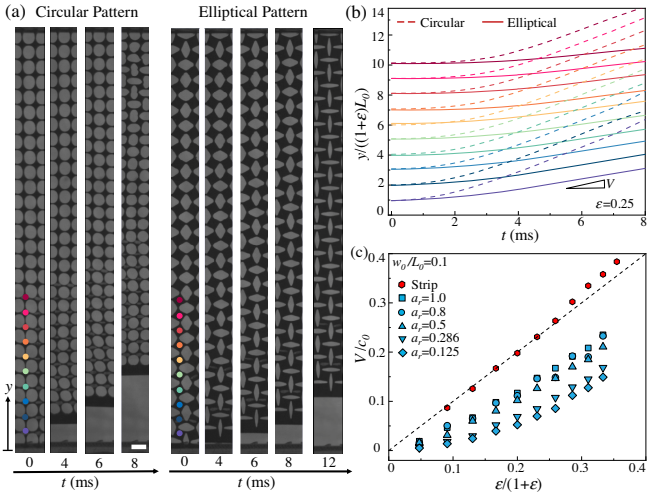

FIG. 3. (a) High-speed images of the elastic recoiling of metamaterials at a strain of 0.25. Scale bar, 5 mm. (b) The positions of plates under elastic recoiling. (c) The normalized recoil velocity as a function of the global strain.

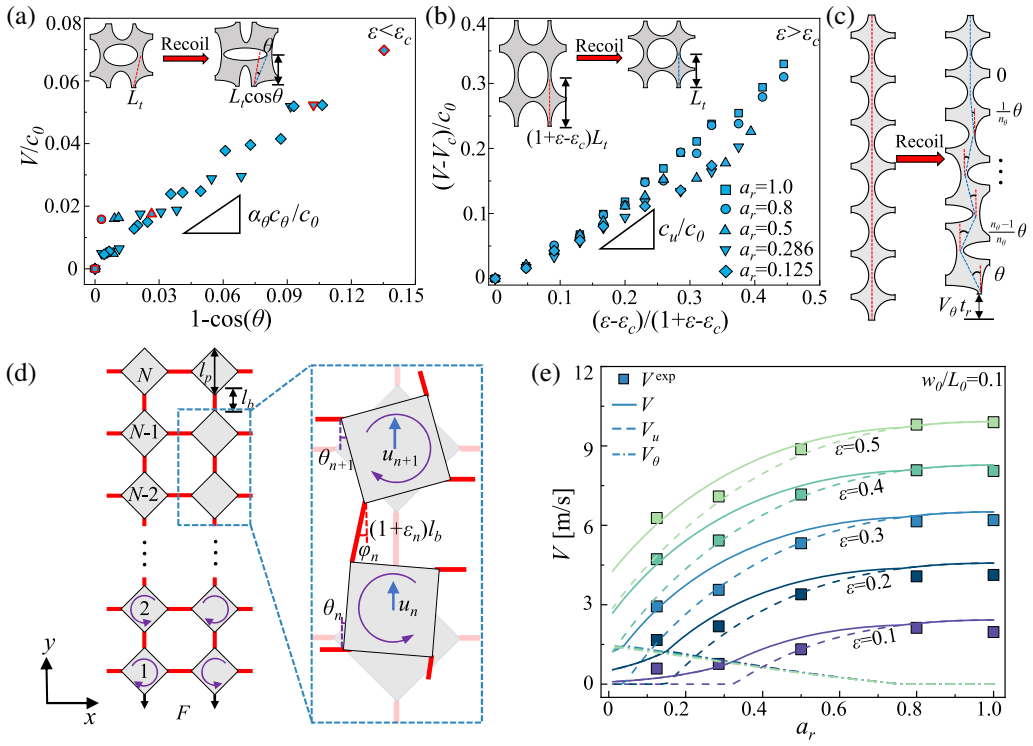

FIG. 4. (a) The recoil velocity depends on the rotational angle when $\varepsilon < \varepsilon_c$. Inset: recoil with rotational displacements. (b) When $\varepsilon > \varepsilon_c$, the recoil velocity is consistent with the strain ratio. Inset: recoil with stretching displacements. (c) Schematic of the plates with decreasing rotational angle in recoil. (d) Plate-chain model of the mechanical metamaterial. (e) Recoil velocities predicted by the model are compared with experimental results.

recoil as the thickness of metamaterials (h) is much larger than ligament width, $h \sim 3w_0$.

We tracked the position of the plates with a marker positioned at the center (Supplemental Material [29]). In Fig. 3(b), the scaled positions corresponding to the color markers in Fig. 3(a) are plotted against the recoiling time. The plates in metamaterials recoil with a constant recoil velocity V, which is the maximum slope in the measured displacement-time curves in Fig. 3(b). The metamaterial with the circular pores recoils around 3 times faster than the one with the elliptical pores.

To establish the relation between the recoil velocity and internal structure, we compared the recoil velocity of metamaterials with different pore shapes [Fig. 3(c)]. The recoil velocity in the strip is dictated by the sound speed in zero-strain limit c_0 and the applied strain ε, $V/c_0 = \varepsilon/(1+\varepsilon)$ [14,16]. The recoil velocities of metamaterials deviate significantly from that of a strip and decrease significantly when the pore shape changes from circular to elliptical, indicating that the internal structure is important in controlling the recoil velocity.

The local displacements in the recoiling metamaterial are manifested as bending and stretching of the ligaments and the rotation and translation of the plates. The rotation angle is zero for circular pores [Fig. 4(a)] and, for elliptical pores, increases until reaching a maximum rotation angle θ_c at a critical strain ε_c (Fig. S5, Supplemental Material [29]). Given that the recoil displacement in each plate due to rotation is about $L_t(1-\cos\theta)$, where L_t is the length between the center of ligaments, the recoil velocity is proportional to $1-\cos\theta$ at $\varepsilon < \varepsilon_c$ [Fig. 4(a)]. To describe the structural control of this rotational recoil velocity V_θ, we consider the metamaterial as a series of rotating squares with rotations propagating at wave speed c_θ. Over a period t_r, a plate rotates an angle θ, and the wave passes n_θ plates, $n_\theta = c_\theta t_r/L_t$ [Fig. 4(c)]. Thus, $V_\theta t_r = \sum_{k=1}^{n_\theta} L_t[1-\cos(k\theta/n_\theta)]$, and

$$V_\theta = \alpha_\theta c_\theta(1-\cos\theta), \tag{1}$$

where α_θ is a geometrically defined constant (see Supplemental Material [29]) of value typically less than unity.

For $\varepsilon > \varepsilon_c$, the recoil velocity increases, even though no further rotation is possible. At larger strains, the metamaterial recoils like a strip, with a strain $\varepsilon - \varepsilon_c$. The proposed mechanism is confirmed in Fig. 4(b) by plotting the rescaled recoil velocity $(V-V_c)/c_0$ against the strain ratio $(\varepsilon-\varepsilon_c)/(1+\varepsilon-\varepsilon_c)$. We adopt V_c as the maximum recoil velocity due to rotation [highlighted in red in Fig. 4(a)] from experiments. Defining V_u as the recoil velocity contributed by stretching, we have

$$V_u = c_u \frac{\varepsilon - \varepsilon_c}{1 + \varepsilon - \varepsilon_c}. \tag{2}$$

The slopes of the recoil velocities in Figs. 4(a) and 4(b) are $\alpha_\theta c_\theta / c_0 \sim 0.6$ and $c_u/c_0 \sim 0.8$, respectively, indicating that the internal displacements propagate with a wave speed differing from the material sound speed c_0.

To confirm this reduced understanding and to generalize the phenomena for different pore shapes, we derived a model that represents the metamaterial as a series of square rigid plates connected by flexible beams [Fig. 4(d)]. Building upon the free energy of the metamaterial in recoil and approximating the discretized field (u_n and θ_n) with a second-order expansion (Supplemental Material [29]), the governing equations of motions are

$$\frac{\partial^2 u}{\partial t^2} - \beta \omega_0^2 L_1^2 \frac{\partial^2 u}{\partial y^2} = 0, \tag{3}$$

$$\frac{\partial^2 \theta}{\partial t^2} - (\alpha - 1)\omega_0^2 L_1^2 \frac{\partial^2 \theta}{\partial y^2} + 8\omega_0^2 \theta = 0, \tag{4}$$

where l_p and l_b are the diagonal lengths of the plates and the length of beams, respectively, and $L_1 = l_p + l_b$. Additionally, $\alpha = C_s[1 + (l_p/l_b)]^2/4C_b$, $\beta = k_l J/mC_b$, and $\omega_0^2 = C_b/J$, where k_l, C_b, and C_s are the stretching, bending, and shearing stiffness of the beam, respectively; m and J are the mass and moment of inertia of the plates, respectively. The length and stiffness of the beam are functions of the global strain, determined by the deformation in the ligament. Further details are found in the Supplemental Material [29].

During the recoil of metamaterials, both the stretching and rotational displacement are activated, and the recoil velocity is $V = V_u + V_\theta$. The wave speeds of the stretching and rotational displacements are predicted by Eqs. (3) and (4). We also predict the critical strain ε_c based on the metamaterial pore aspect ratio via a kinematic model (Supplemental Material [29]). In Fig. 4(e), we plot the recoil velocity for pores with aspect ratio a_r ranging from 0 to 1 and find good agreement with experiments. The recoil velocity monotonically increases with a_r for all strains, as the stiffness and the corresponding strain energy increases with a_r. When $\varepsilon < \varepsilon_c$, the metamaterial only undergoes rotational displacement in recoil; when $\varepsilon > \varepsilon_c$, the metamaterial recoils with translational displacements first, followed by rotation. The sequential unloading allows for the modulation of the recoil velocity with internal structures.

Most synthetic materials experience intrinsic dissipation that is amplified at high strain rates [17–19]. In the elastic recoil, the strain energy stored in the quasistatic loading W_s is not fully converted to kinetic energy in recoil, $W_k = \frac{1}{2} mV^2$. For a nonstructured strip, the energy conversion ratio W_k/W_s decreases with the global strain [Fig. 5(a)]. The dissipation is amplified at high strain, as confirmed in the inset of Fig. 5(a), where the decay of W_k/W_s with the strain $(1 + \varepsilon)$ is of the order -2 [35]. For metamaterials, the dissipation is nonmonotonic with respect to the global strain and depends on the pore aspect ratio, showing an optimized value featuring small a_r.

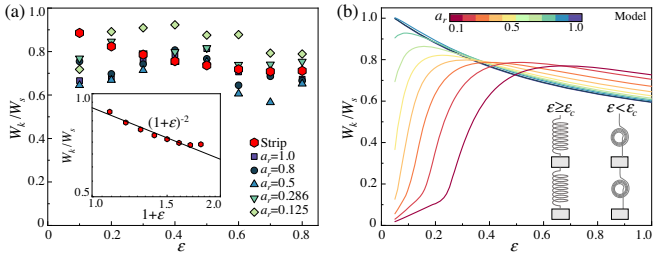

FIG. 5. (a) Energy conversion ratio in both the nonstructured strip and metamaterials. Inset: experimentally observed decay in a strip. (b) Energy conversion ratio predicted by the model. Inset: harmonic oscillator with tensional and rotational springs.

To demonstrate that this optimized enhanced efficiency is programmed by the metamaterial stiffness and local displacements, rather than other potential sources of dissipation (e.g., friction during release), we plot the energy conversion ratio predicted by our model in Fig. 5(b). Similar to the trend observed in experiments, our model indicates a nonmonotonic trend of energy conversion ratio in metamaterials with the presence of rotational displacements. An optimized enhanced efficiency also features smaller a_r as the global strain increases. To understand the structural origin of dissipation, we simplify the metamaterial in elastic recoil as a series of spring-mass oscillators [36] [inset, Fig. 5(b)]. When $\varepsilon > \varepsilon_c$, the metamaterial is governed by tension springs. The energy conversion ratio follows $W_k/W_s \sim k_l(\varepsilon)/\langle k_l(\varepsilon)\rangle$, where $\langle k_l(\varepsilon)\rangle = \varepsilon^{-2} \int_0^\varepsilon k_l(\gamma)(\gamma)^2 d\gamma$ is the average stiffness during the quasistatic loading [37]. The dissipation is controlled by the dependence of stiffness upon strains in metamaterials. When $\varepsilon < \varepsilon_c$, the metamaterial response is dominated by rotational springs. The energy conversion ratio follows $W_k/W_s \sim (1 - \cos\theta)^2$, which increases with global strain until reaching the maximum rotational angle at $\varepsilon = \varepsilon_c$ [38]. Despite mechanical interactions being more complex in the metamaterials, the physical picture emerging from the model points to the essential role of the internal displacements.

In summary, we have studied the asymmetric loading and unloading in impulsive deformation with mechanical metamaterials. The designed internal structures incorporate slender ligaments that permit rotation of more rigid plates and control the localized displacements via the pore geometry. Our results indicate that asymmetric quasistatic loading and the impulsive unloading are programmed with tunable stiffness and recoil velocity, respectively. More importantly, the internal structures in the metamaterial control the energy conversion process. Different from experimentally observed decay with the global strain observed in the continuous materials, the energy conversion efficiency in the metamaterial is determined by the internal

displacements. Thus, the internal structure allows the force, velocity, power, and dissipated energy to be tuned to match performance needs and constraints in impulsive recoil.

This work is supported by the U.S. Army Research Laboratory and the U.S. Army Research Office under Contract No. W911NF-15-1-0358. The authors thank Professor Ryan Hayward for use of the high-speed camera.

*Corresponding author.
acrosby@umass.edu

[1] M. Ilton *et al.*, Science **360**, eaao1082 (2018).
[2] M. Burrows, Nature (London) **424**, 509 (2003).
[3] R. M. Alexander and H. Bennet-Clark, Nature (London) **265**, 114 (1977).
[4] M. H. Dickinson, C. T. Farley, R. J. Full, M. Koehl, R. Kram, and S. Lehman, Science **288**, 100 (2000).
[5] S. Patek, W. Korff, and R. Caldwell, Nature (London) **428**, 819 (2004).
[6] T. Zack, T. Claverie, and S. Patek, J. Exp. Biol. **212**, 4002 (2009).
[7] S. Longo, S. Cox, E. Azizi, M. Ilton, J. Olberding, R. St Pierre, and S. Patek, J. Exp. Biol. **222**, jeb197889 (2019).
[8] Y. Forterre, J. M. Skotheim, J. Dumais, and L. Mahadevan, Nature (London) **433**, 421 (2005).
[9] M. Escalante-Pérez, E. Krol, A. Stange, D. Geiger, K. A. Al-Rasheid, B. Hause, E. Neher, and R. Hedrich, Proc. Natl. Acad. Sci. U.S.A. **108**, 15492 (2011).
[10] P. E. Klopsteg, Am. J. Phys. **11**, 175 (1943).
[11] S. Ranallo, C. Prévost-Tremblay, A. Idili, A. Vallée-Bélisle, and F. Ricci, Nat. Commun. **8**, 15150 (2017).
[12] P. Mason, J. Appl. Phys. **31**, 1706 (1960).
[13] B. A. Mrowca, C. L. Dart, and E. Guth, Phys. Rev. **66**, 30 (1944).
[14] R. Vermorel, N. Vandenberghe, and E. Villermaux, Proc. R. Soc. A **463**, 641 (2006).
[15] J. Niemczura and K. Ravi-Chandar, J. Mech. Phys. Solids **59**, 423 (2011).
[16] A. T. Oratis and J. C. Bird, Phys. Rev. Lett. **122**, 014102 (2019).
[17] M. Ilton, S. Cox, T. Egelmeers, G. P. Sutton, S. Patek, and A. J. Crosby, Soft Matter **15**, 9579 (2019).
[18] J. Niemczura and K. Ravi-Chandar, J. Mech. Phys. Solids **59**, 457 (2011).
[19] R. Bogoslovov and C. Roland, J. Appl. Phys. **102**, 063531 (2007).
[20] M. Burrows and G. P. Sutton, J. Exp. Biol. **215**, 3501 (2012).
[21] S. Patek, M. Rosario, and J. Taylor, J. Exp. Biol. **216**, 1317 (2013).
[22] D. Raabe, C. Sachs, and P. Romano, Acta Mater. **53**, 4281 (2005).
[23] K. Bertoldi, V. Vitelli, J. Christensen, and M. van Hecke, Nat. Rev. Mater. **2**, 17066 (2017).
[24] H. Yasuda, L. M. Korpas, and J. R. Raney, Phys. Rev. Applied **13**, 054067 (2020).
[25] B. Deng, J. R. Raney, V. Tournat, and K. Bertoldi, Phys. Rev. Lett. **118**, 204102 (2017).
[26] B. Deng, C. Mo, V. Tournat, K. Bertoldi, and J. R. Raney, Phys. Rev. Lett. **123**, 024101 (2019).
[27] X. Liang and A. J. Crosby, Extreme Mech. Lett. **35**, 100637 (2020).
[28] N. Gao, J. Li, R. Bao, and W. Chen, Soft Matter **15**, 2921 (2019).
[29] See Supplemental Material at http://link.aps.org/supplemental/10.1103/PhysRevLett.125.108002 for material properties and geometric parameters of metamaterials used in experiment, as well as additional details of the high-speed imaging analysis and the derivation of the reduced model for the recoil dynamics and dissipation. Videos of the elastic recoil are also included. The Supplementary Materials include Refs. [30,31].
[30] D. Brown and A. J. Cox, Physics Teacher **47**, 145 (2009).
[31] I. Jasiuk, J. Chen, and M. Thorpe, Appl. Mech. Rev. **47**, S18 (1994).
[32] C. Coulais, Int. J. Solids Struct. **97**, 226 (2016).
[33] C. Coulais, C. Kettenis, and M. van Hecke, Nat. Phys. **14**, 40 (2018).
[34] L. J. Gibson and M. F. Ashby, *Cellular Solids: Structure and Properties* (Cambridge University Press, Cambridge, United Kingdom, 1999).
[35] For the elastic recoil of a rubber band, dissipation is embedded in the relation between the recoil velocity and the wave speed in recoil. It follows $W_k/W_s \sim \frac{1}{2}\rho V^2/\frac{1}{2}E\varepsilon^2 \sim (1+\varepsilon)^{-2}$, where E_0 and ρ_0 are the elastic modulus and density, respectively, and the recoil velocity $V = \varepsilon(1+\varepsilon)^{-1}\sqrt{E_0/\rho_0}$ based on dynamics of an elastic strip.
[36] G. Ma and P. Sheng, Sci. Adv. **2**, e1501595 (2016).
[37] For $\varepsilon > \varepsilon_c$, the metamaterial undergoes both local rotation and stretching, and the stiffness of the metamaterial varies with the applied strain, $k_l = k_l(\varepsilon)$. Therefore, the strain energy stored in the quasistatic loading is $W_s \sim \int_0^\varepsilon \frac{1}{2}k_l(\gamma)(L_0\gamma)^2 d\gamma$. The metamaterial is represented by the translational harmonic oscillator with an amplitude of $A = L_0\varepsilon$ in the recoil direction, and the period of oscillation is $T = 2\pi\sqrt{m/k_l(\varepsilon)}$. Therefore, the recoil velocity is scaled by $V \sim A/T \sim L_0\varepsilon\sqrt{k_l(\varepsilon)/m}$. The kinetic energy is scaled as $W_k \sim \frac{1}{2}k_l(\varepsilon)\varepsilon^2 L_0^2$. It follows $W_k/W_s \sim k_l(\varepsilon)\varepsilon^2/\int_0^\varepsilon k_l(\gamma)(\gamma)^2 d\gamma$.
[38] For $\varepsilon < \varepsilon_c$, the metamaterial only undergoes the local rotation. We estimate the strain energy by neglecting the change of the bending stiffness C_b in small strains, $W_s \sim \frac{1}{2}C_b\theta^2$. The metamaterial is represented by the rotational harmonic oscillator with an amplitude of $A = L_0(1-\cos\theta)$ in the recoil direction, and the period of oscillation is $T = 2\theta\sqrt{J/C_b}$. The recoil velocity is scaled by $V \sim A/T \sim L_0\theta\sqrt{C_b/J}(1-\cos\theta)$. The kinetic energy is scaled as $W_k \sim \frac{1}{2}(mL_0^2/J)C_b\theta^2(1-\cos\theta)^2$. It follows $W_k/W_s \sim (1-\cos\theta)^2$.